

Overcoming Limitations in the Automated Mass Production of Optical Instruments

Christopher Schindlbeck

Institute of Measurement and Automatic Control, Leibniz Universität Hannover

Nienburger Str. 17, 30167 Hannover, Germany

E-Mail: christopher.schindlbeck@imr.uni-hannover.de

Abstract

While automated mass production is gradually advancing in many fields (such as the automobile industry), this leap has not been made yet in the assembly of optical instruments. Nowadays, optical instruments integrate active or passive adjustment mechanisms for each critical optical component to maintain the high demands on tolerances (such as in interferometric devices) in order to preserve the system's functionality. In turn, this leads to increased production and labor costs.

In this paper, several approaches are proposed to overcome these problems from a hardware and software perspective to yield a more cost-efficient solution and to make progress towards an automated mass production. To lower the overall system cost while increasing workspace size and positioning accuracy, a macro-micro-manipulator can be employed. By choosing a certain control strategy, the tight alignment tolerances of interferometers can be furthermore lowered. For geometrically simple interference pattern that arise e.g. in a Michelson interferometer, an image-based approach via extraction of center points is presented. For more complicated interference pattern, two machine learning approaches are investigated.

Introduction

Interferometric devices are amongst the most precise optical metrology instruments. They can be employed in fields such as length measurement, high-resolution spectroscopy, and optical component testing. However, these devices are prone to a large variety of error sources [1] which may lead to partial or even full loss of functionality. These error sources are mainly:

- (i) Geometric beam misalignment
- (ii) Wavefront deformations such as aberrations
- (iii) Loss of beam intensity
- (iv) Changes in the laser-wavelength of the light source
- (v) Change in polarization direction

Due to lacking methods to cope with these errors, an automated mass production of interferometers can not be realized yet.

One of the greatest challenges in the assembly of interferometric devices is to maintain the tight alignment tolerances (i) to preserve their full functionality. Interferometric devices may require absolute positioning accuracies in the nanometer range. Furthermore, optical components are subject to production errors which lead to either non-ideal surfaces or inhomogeneous material (ii).

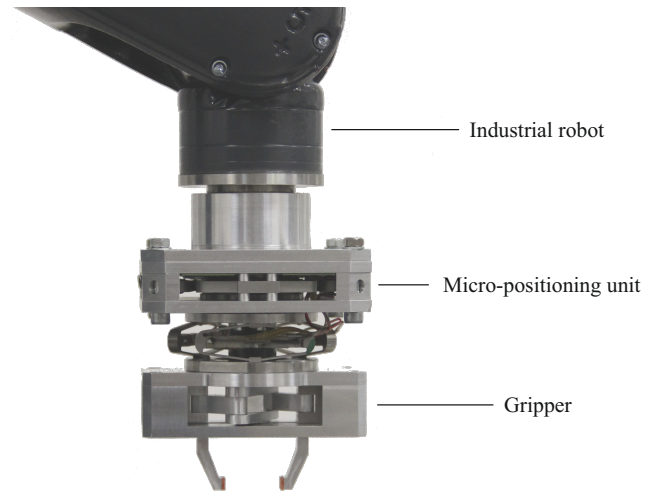


Figure 1: Industrial robotic manipulator augmented with high-precision micro-positioning unit and gripper for grasping optical components.

This needs to be considered as well in the assembly process. Error sources such as the choice of high-quality beam sources (iii) as well as component aging and environmental changes (iv) only play a subordinated role in the assembly process and need to be addressed accordingly before or after assembly, respectively. Therefore, they will not be considered here. The current industrial solution is to integrate adjustment mechanisms for each optical component [2] and having an expert manually adjusting components after assembly to guarantee functionality. In turn, this leads to increased production and labor costs. Although the integration of active adjusting mechanisms has been proposed (see e.g. [3]) to reduce labor costs, the increased production costs still persist or are even worse due to (relatively expensive) active mechanisms.

In this paper, two strategies are outlined that are suitable for overcoming the problems of error sources for assembly processes in optical instruments. First, a method to increase the accuracy of industrial robotic manipulators is outlined. Low-cost industrial robotic manipulators have low precision and a large workspace, while expensive high precision machines have opposing characteristics. In order to overcome the problem of workspace size limitations and the low precision of serial manipulators, they can be augmented by a micro-positioning unit that alleviates the aforementioned problems. This results in a so-called macro-micro-manipulator. Secondly, strategies to reduce the demands on absolute placement precision of optical components are outlined. The idea is, instead

of trying to place components as accurately as possible, to use the interference pattern as quantity of interest for the placement of optical components. In this paper, interference pattern that arise in a misaligned Michelson interferometer (so-called Haidinger fringes) are analyzed. A segmentation-based technique is presented to infer the mirror tilt from the nominal case (centered circles). On the other hand, wavefront aberrations are present in real optical components and therefore a classification method is presented such that this can be used as basis for future alignment experiments.

Macro-Micro-Manipulation

The industrial robot *KUKA Agilus KR10 R1100 sixx* serves as macro-positioning system with a repetition accuracy of only 0.03 mm which is clearly orders of magnitude away from a precision required in optical systems. Therefore, the 3-degrees-of-freedom positioning stage *XYZ200M* from *Cedrat Technologies* driven by piezoelectric actuators is used as micro-positioning unit to augment the manipulator. It weighs about 540 g with a nominal displacement of 200 μm and a (nominal) blocked-force of 118 N in each Cartesian direction with a nanoscopic resolution of 2 nm. A National Instruments real-time system is used to command voltage input and access strain-gauge measurements for control purposes. Piezoelectric actuators inherently suffer from nonlinear characteristics (mainly hysteresis and creep effects) which need to be addressed by appropriate control strategies. In [4], [5] a model-based feedforward controller for the compensation of these characteristics was presented.

The augmented macro-micro-manipulator is equipped with a gripper that enables pick-and-place tasks for the assembly process. Since optical components are delicate objects, the application of high forces during the grasping process should be avoided. Therefore, control methodologies with active compliance such as impedance control are particularly suited. The entire system consisting of the industrial manipulator, the micro-positioning unit, and the gripper is depicted in Fig. 1. This proposed system is capable of placing optical components during the assembly of optical instruments such as a Michelson interferometer. In the upcoming sections, simulations are carried out to investigate the influence of misaligned components during the assembly process.

Simulation of a Michelson Interferometer

In this paper, a simple Michelson interferometer (see Fig. 2) is simulated to analyze the effects of misaligned components. A collimated light source with circular aperture of diameter $2R$ transmits monochromatic light with wavelength λ through a lens with focal length f . The light beam hits a beamsplitter (BS) after distance z_1 and transmits / refracts two amplitude-partitioned light beams with an amplitude ratio of R_{BS} . One part is propagated to mirror 1 (reference mirror) in distance z_3 and the other part is propagated to mirror 2 (moving mirror) in distance z_2 . Both light beams are reflected in a lossless

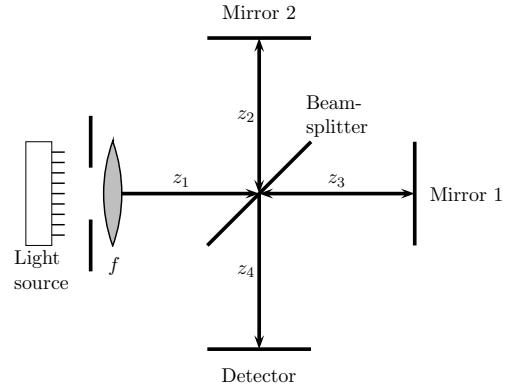


Figure 2: Simplified model of a Michelson interferometer.

Wavelength λ	500 nm
Distance lens - BS z_1	10 cm
Distance BS - moving screen z_2	50 cm
Distance BS - reference screen z_3	30 cm
Distance BS - CCD screen z_4	10 cm
Aperture radius r_0	12 cm
Screen size s	25 cm
Screen pixel density	$20 \cdot 10^3 \frac{\text{px}}{\text{m}}$
Focal length f	600 cm
BS transmission / refraction ratio R_{BS}	0.5

Table 1: Parameters for the simulated Michelson interferometer used in the experiments.

manner back to the BS and where they are recombined again. Afterwards, the combined beam is propagated to the screen in distance z_4 from the BS where a screen is placed.

For the alignment problem, the reference mirror is tilted by an angle to produce off-center interference pattern while the moving mirror is fixed. For the classification problem, both mirrors are fixed but mirror 2 is overlaid by wavefront aberrations. The beam propagation toolbox *LightPipes* is utilized for the simulation of the interferometer and the respective parameters for the simulations are listed in Tab. 1. In the next sections, the simulation will be used to analyze the effect of rotational misalignments and wavefront aberrations present in a mirror.

Extraction of Center Points

In this section, a sequential approach for the extraction of center points of misaligned Haidinger fringes is presented. The proposed strategy is as follows:

1. Image pre-processing (binarization and removal of artifacts)
2. Finding connected components
3. Fitting circles to connected components (via e.g. Hough-Transformation)
4. Applying an iterative contraction algorithm to find correct center points

In the first step, a binary image of the interference pattern is obtained. This is done by selecting an appropriate threshold. Afterwards, remaining artifacts due to binarization are discarded by a 4-connectivity approach.

A [rad]	Piston	Tilt	Defocus	Astigmatism	Coma	Spherical
$A = 5.0000$						
$A = 6.4286$						
$A = 7.8571$						
$A = 9.2857$						

Table 2: Interference pattern generated by primary lens aberrations and a variation of the phase shift A .

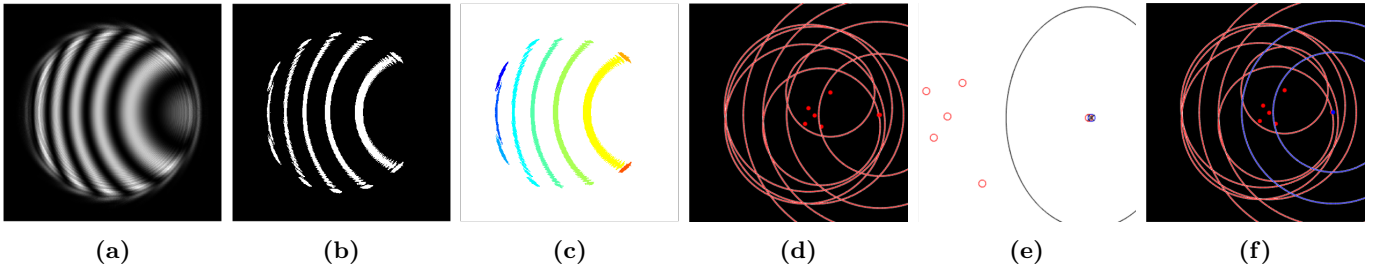


Figure 3: Sequential center point extraction for circular interference pattern: Original interference pattern (a), binary image (b), connected components (c), fitted circles to each component (d), results of iterative algorithm (e), and final center extraction (f).

The next step finds connected components by using an 8-connectivity approach. Then, a circle can be fitted to each connected component which leads to a set of center points. An iterative contraction algorithm¹ is then applied to find the correct center point that corresponds to the displaced interference pattern. Fig. 3 depicts each of the aforementioned steps. This strategy can then be used in combination with a Kalman filter for feedback control, see Fig. 4. Based on the off-centered center points, a controller can be laid out which gives input to the robotic system in order to align optical components.

Classification of Wavefront Aberrations

Interferometric devices that analyze areal surfaces (such as in optical component testing) instead of isolated points produce different and more complicated interference pattern than the simple Michelson interferometer with its

¹For sake of brevity, this algorithm will not be described here and will be submitted to a future publication.

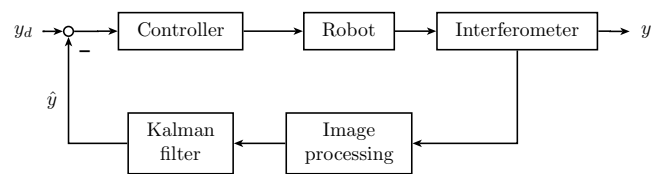


Figure 4: Schematic for proposed feedback control in assembly processes of optical instruments.

Haidinger fringes. For this, a more general strategy than the one proposed in the last chapter needs to be developed. In this paper, a machine learning approach is proposed to tackle the problem. Here, surface deformations are simulated via six low-order wavefront aberrations. A variety of interference pattern for different primary wavefront aberrations is depicted in Tab. 2. Therein, A is the corresponding phase shift of the aberra-

tion. For the classification of wavefront aberrations, two state-of-the-art algorithms are compared, Support Vector Machines (SVM) and Convolutional Neural Networks (CNN). SVM [6] are large-margin classifier which can also be used to solve regression problems. CNN [7] are especially suited for image recognition and classification since they take into account local spatial correlations of images and therefore exploit certain invariance properties. This is achieved by the incorporation of local receptive fields, shared weights, and pooling (also: subsampling) [8]. CNN consist of a purely feedforward layered architecture comprised of alternating convolution and pooling layers which finalizes with a multilayer perceptron. The name is derived from the discrete convolutions in the respective layers.

Before applying the SVM algorithm, pre-processing of the feature space is performed by normalized the data set to $[0, 1]$. The feature vector \mathcal{F} is constructed from rotational invariant image descriptors $|Z_{nm}|$ such that

$$\mathcal{F} = (|Z_{00}|, |Z_{11}|, |Z_{20}|, |Z_{22}|, |Z_{31}|, |Z_{40}|)^T.$$

Here, Z_{nm} are Zernike or Pseudo-Zernike polynomials with corresponding indexing. Of course, higher-order terms could be integrated to improve the classification performance. However, the feature vector is purposely kept low to correspond to the classification features. For our SVM design the C-support vector classification [6] is chosen, where a penalizing parameter C is applied for both classes. A Gaussian radial basis function kernel $K(x, x') = \exp(-\gamma\|x - x'\|^2)$ with x and x' as inputs is used for classification with γ as kernel parameter. LIB-SVM [9] is used for the simulation with $\gamma = n_f^{-1}$, where n_f is the number of features (here: $n_f = 6$) and $C = 10$. For CNN, the data set needs to be pre-processed as well (similar to SVM approach) in order to yield better classification performance. Here, the data is transformed such that it has zero mean $\mu = 0$ and a unit standard deviation $\sigma = 1$. Furthermore, the data is reduced to have 32-by-32 pixels to fit the architecture. The CNN architecture is chosen according to LeNet-5 [7] except here 6 outputs and the tan-sigmoid as activation function is chosen.

The simulation results after a 5-fold cross validation are depicted in Fig. 5. Therein, the recognition rate is shown for each of the aforementioned approaches. These preliminary results show that SVM with Pseudo-Zernike polynomials yield better results than SVM with Zernike polynomials but CNN outperform both methods.

Conclusion and Outlook

In this paper, strategies to overcome the limitations for an automated mass production of optical instruments were presented. Increasing the workspace and placement accuracy, while simultaneously keeping the costs low can be realized for example with a macro-micro-manipulator. In order to lower the demands on placement accuracy, image-based feedback control techniques can be applied. For tilting displacement, feedback by the center points of the interference pattern can be employed as feedback strategy. For the classification of wavefront aberrations,

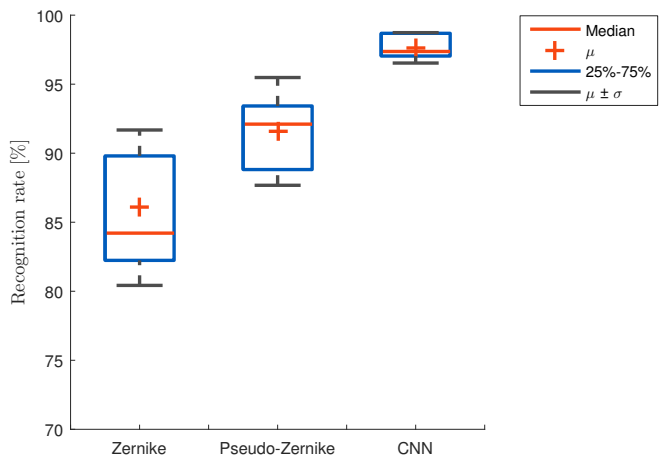


Figure 5: Classification results for wavefront aberrations.

three approaches were compared and CNN yielded the best performance w.r.t. to recognition rate. In future work, experiments are to be conducted by combining software-based feedback techniques as presented on the macro-micro-manipulator.

References

- [1] A. Bai, F. Bitte, H. K. Mischo, and T. Pfeifer, “Interferometer calibration: an approach with the virtual interferometer,” in *International Symposium on Optical Science and Technology*. International Society for Optics and Photonics, 2000, pp. 502–509.
- [2] R. E. Abbink, “Interferometer alignment,” Oct. 4 2005, US Patent 6,952,266.
- [3] C. G. Prevost and J. Genest, “Dynamic alignment of a michelson interferometer using a position-sensitive device,” in *Proc. of the SPIE 49th Annual Meeting*. International Society for Optics and Photonics, 2004, pp. 293–304.
- [4] C. Schindlbeck, C. Pape, and E. Reithmeier, “Recursive online compensation of piezoelectric nonlinearities via a modified prandtl-ishlinskii approach,” in *Proc. of the 20th IFAC World Congress, Toulouse*, 2017.
- [5] —, “Two degree-of-freedom online compensation of a piezoelectric micro-positioning unit,” in *Proc. Appl. Math. Mech*, 2017.
- [6] C. Cortes and V. Vapnik, “Support-vector networks,” *Machine Learning*, vol. 20, no. 3, pp. 273–297, 1995.
- [7] Y. LeCun, L. Bottou, Y. Bengio, and P. Haffner, “Gradient-based learning applied to document recognition,” *Proc. IEEE*, vol. 86, no. 11, pp. 2278–2324, Nov 1998.
- [8] C. M. Bishop, *Pattern Recognition and Machine Learning*. Singapore: Springer, 2006.
- [9] C.-C. Chang and C.-J. Lin, “Libsvm: A library for support vector machines,” *ACM Trans. Intell. Syst. Technol.*, vol. 2, no. 3, pp. 27:1–27:27, May 2011.